



# Numerical Study of the Force Transfer Mechanism and Seismic Behavior of Masonry Infilled RC Frames with Windows Opening

Ebrahim Khalilzadeh Vahidi <sup>a\*</sup>, Reza Moradi <sup>b</sup>

<sup>a</sup> Assistant Professor, Razi University, Kermanshah, Iran.

<sup>b</sup> MSc Student in Civil Engineering, Razi University, Kermanshah, Iran.

Received 16 June 2018; Accepted 07 December 2018

## Abstract

Masonry infilled walls are widely used in reinforced concrete (RC) frames worldwide. However, infilled RC frame building failure is a common mode in destructive earthquakes. Further researcher is needed to bring insightful understandings into the behaviors of these structures. Therefore, this study investigates seismic parameters, ultimate tensile damage, and force transfer mechanisms in a reinforced concrete structure under in-plan load. For this purpose, the definitions and the relevant literature were reviewed. Then, an analytical software supporting an infill model was selected and described altogether with a particular modeling approach. Calibrating software results with those presented by Abdulhafez et al. (2014), the researchers designed a series of planer one-story one-bay reinforced concrete frames upon ACI 318M-14 Building Code. The seismic behavior of infilled frames were also studied using finite element method. Force transfer mechanisms in infilled frame with opening, which is one of the important items, was investigated in this study. Comparing the analysis outcomes with the bar frame, it was indicated that the ultimate load, stiffness, and toughness of the full in-filled frame were increased while the ductility was decreased. It was also revealed that the presence of opening in infilled frame decreased the ultimate load, stiffness and toughness corresponding full infilled frame. In addition, the increasing of opening size increased the reduction of the ultimate load, stiffness and toughness.

**Keywords:** Pedestrian Two-Stage Crossing; Route Choice; Pedestrian Behavior Model; Signalized Intersections.

## 1. Introduction

Recently, an established body of research has investigated the seismic behavior of RC frames under earthquake excitation. Studying this behavior is critically significant since this issue has received little attention in the current building codes. Infilled frame is a panel, which partly or fully covers a steel or RC frame, and it is surrounded by grid of beams and columns. Infilled frame is considered as a partition or an infilled wall, which is filled with a panel of another material, such as brick or hollow concrete-blocks [1]. Concrete frame structure with masonry is the common type of construction technology applied in some parts of the world, particularly in developing countries. It is easy to build and attractive for architecture. Masonry infilled frames could have positive or/and negative impacts on RC structures. Hence, they can influence the seismic behaviours including ductility, ultimate strength, stiffness, toughness in a way that it may be impossible to describe the compound characteristics of the frame by summing up its properties. Masonry infilled frame is usually ignored in designing a concrete structure despite its significance on concrete structures. Therefore, this study could provide us with insightful understandings of how the concrete structure might response to the earthquake excitations [2].

\* Corresponding author: e\_vahidi2000@yahoo.com

<http://dx.doi.org/10.28991/cej-2019-03091225>

➤ This is an open access article under the CC-BY license (<https://creativecommons.org/licenses/by/4.0/>).

© Authors retain all copyrights.

Since past decades, a body of research has evaluated the seismic behaviour of frames with masonry infill. In a more recent investigation, Hapsari et al., (2018) [3] studied an irregular four-story RC building with and without masonry infills using nonlinear static procedure. They observed that the lateral strength of RC building with masonry infills was higher than RC building without masonry infills. In contrast, the amount of damage to RC building with masonry infills was lower than RC building without masonry infills. Alwashali et al., (2018) [4] investigated the backbone curve and deformation of masonry infilled RC frames. For this purpose, they tested two infilled RC frames. Experimental results indicated that the increase in frame's shear strength, which was relative to the shear strength of the infilled wall, increased the strength and betterment of the sudden brittle behavior of the infilled frame. In a series of experiments, Syed and Hemant (2016) [5] studied the behavior of eleven half-scale masonry infilled RC frames under cyclic in-plane loading. The results illustrated that an idealized load-displacement relationship was developed for masonry infilled RC frames in different performance levels. The study also showed that, in most of the specimens, column failed in shear although the used masonry wall was quite weak. Chen and Liu (2016) [6] investigated the effects of vertical loads on in-plane behaviours of infilled wall covered by reinforced concrete frames. Using Ansys software, the researchers modelled four specimens of infilled frames and applied lateral loads to these samples. They also modelled six further specimens. These frames were tested under both vertical and lateral loadings. The limit analysis of infill wall showed that the effect of vertical loading on stiffness and resistance was depended upon the aspect ratio of infill wall, the smaller the height of the infilled wall, the higher the amount of stiffness and resistance.

Kiani et al., (2016) [7] investigated the fragility curves of reinforced frames with semi-rigid saddle connections. In this semi-rigid connection, the main things were placed on each side of the column. Two splints were welded at the top and bottom of the beams. The secondary beams, which were stood vertically on the plates of these frames and connected to the primary beams, function as the bases for brick wall floors. Kiani et al. used three lateral load systems including, masonry infill walls, concentric braces, and a combination of concentric bracings and a combination of concentric braced frames with masonry infill walls in order to investigate the seismic behavior and vulnerability assessment of steel structures in three - and five-story steel structures. These researchers utilized OpenSees software for numerical modeling and structural analyses. Observing pushover and hysteretic curves, Kiani et al. concluded that "steel frames only without any bracing system or with infill walls only ... [were] very damageable due to the premature failure of the infills which result in sudden strength and stiffness degradation in the system". It was also observed that soft story formation occurred in the lowest story. In another study, Yuen and Kuang (2015) [8] investigated the seismic performance and failure mechanisms of two-story two-bay masonry infilled RC frames under dynamic loading. The results showed that the infill walls crucially affected the seismic behavior of RC frames. The analysis also showed that the design concept of "strong column-weak beam" may not be always enforceable to infilled RC frames.

Tawfik Essa et al., (2013) [9] further investigated the effect of masonry infill wall on the performance of high strength RC frames. They conducted experiments on four half-scale, single-story single-bay under cyclic loading. They mainly concluded that the ultimate resistance for infilled RC frames was greater than the bar frame. Okuyucu (2010) [10] also studied the influence of aspect ratio of the RC frames on the precast concrete wall strengthening method. She conducted test on fifteen 1/3 scale infilled RC frames. Results showed that the precast concrete wall application remarkably increased the ultimate resistance of the reinforced concrete frames. In a further study, Akin (2011) [11] investigated the experimental behavior of eight 1/3 and four 1/2 scale infilled RC frames with several aspect ratios. It was shown that the initial stiffness and ultimate resistance of the infilled RC frames increased remarkably. Baran and Sevil (2010) [12] also tested three 1/3 scale one-story one-bay and five 1/3 scale two-story one-bay masonry infilled RC frames by changing axial load on columns, lap-splicing and mortar strength. They observed that the ultimate resistance and stiffness of the infilled RC frames increased in comparison to bare frames.

## 2. Research Methodology

In the continuation of the contextualized studies, this study examined the effect of window opening on seismic behavior of RC frames. First, the relevant studies were reviewed. Second, in order to attest the results, Abaqus software was used to model the laboratory experiment of Lyla Abol-Hafiz et al. (2014) [13], and the results were compared. Third, a RC frame was designed upon ACI code. The thickness of the wall, its characteristics, and opening dimensions were also determined. Forth, six specimens including, bar frame, one fully infilled frame, and five in-filled frames respectively with 10, 20, 30, 40 and 50 percent opening, were modelled and analyzed using ABAQUS software. Finally, the parameters of force transfer mechanism, impact of tensile force on patterns of cracks, ultimate strength, initial stiffness, ductility, and toughness were investigated.

## 3. Infilled RC Frame Prototype Structure

The prototype structure is a one-story one-bay RC building frame designed by ACI 318M-14. The uniaxial strengths of the longitudinal, transverse reinforcements and concrete are 300 MPa, 300 MPa and 32 MPa, respectively. The infilled frames are composed of 300-mm-thick infill panels with 7.5 MPa compressive strength and 10-mm-thick mortar joints with 1.7 MPa compressive strength. Seven typical types of masonry-infill classification are considered in this study: (1)

bar frame, (2) full infill, (3) infill with 10% window opening, (4) infill with 20% window opening, (5) infill with 30% window opening, (6) infill with 40% window opening, and (7) infill with 50% window opening. The windows opening is located in the center of the wall. The reinforcement details and specimens' dimension are shown in Figure 1.

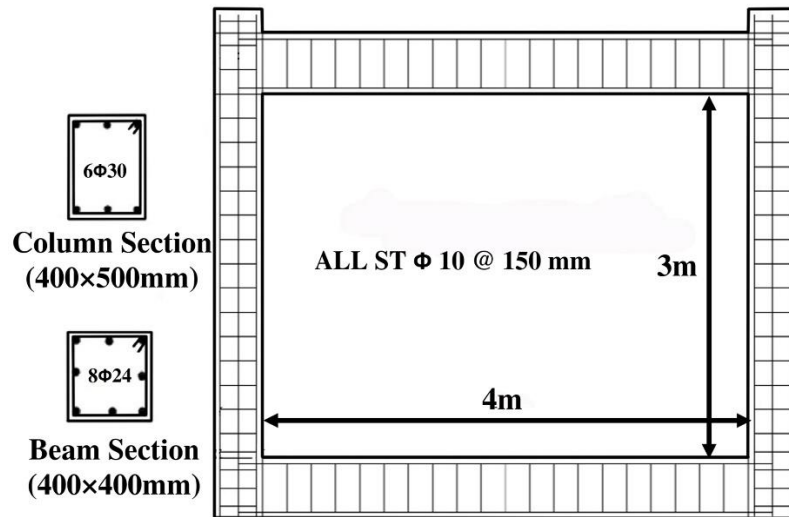


Figure 1. Reinforcement details and specimens dimension

#### 4. Finite Element Modeling

The finite element method (FEM) or finite element analysis (FEA) is a powerful tool that can be used to investigate the seismic performance of infilled RC frames under lateral loading [14]. From the computational point of view, the finite element modeling techniques used for the analysis of masonry wall can be divided into three main categories : (1) detailed micro-model, (2) simplified micro-model, and (3) macro-model (Figure 2)[15].

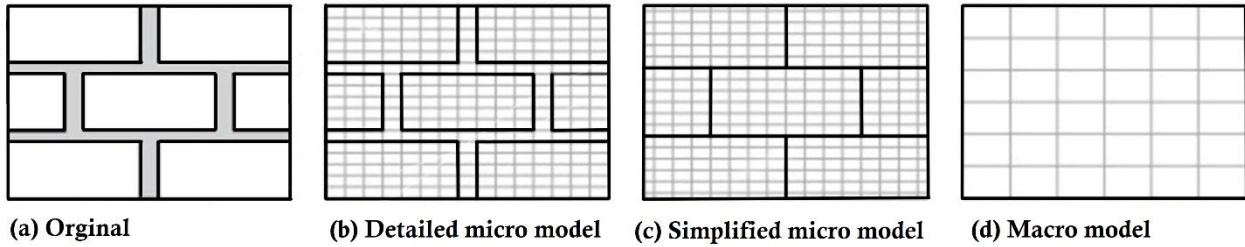
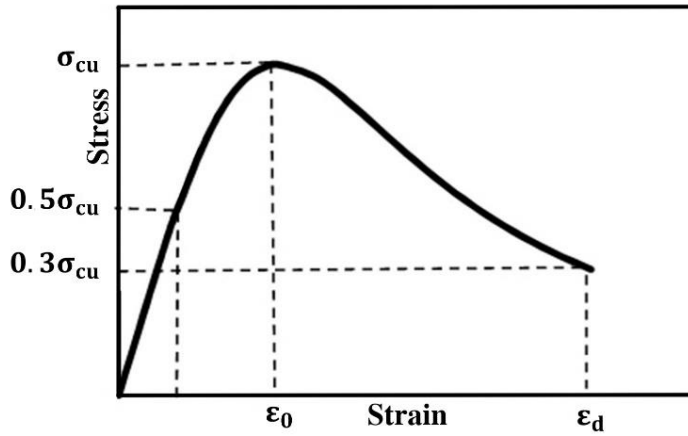


Figure 2. masonry modeling strategist [15]

##### 4.1. Material Characteristics of the Concrete

The plastic-damage model in ABAQUS software is utilized to simulate the behavior of concrete material in columns and beams. Concrete Damage Plastic (CDP) model has been used to predict the conduct of concrete and other quasi-brittle materials, such as mortar and rock under different loading conditions. Crushing in compression or cracks in tension are the principal damage modes to this model [16]. The model developed by Hsu and Hsu (1994) [17] is selected for this study (Figure 3). This model is considered appropriate for the evaluation of compressive behavior of the concrete. This model can be used to develop the stress-strain relationship under uni-axial compression up to  $0.3\sigma_{cu}$  of stress in the descending portion, only using the maximum compressive strength ( $\sigma_{cu}$ ). In the next section, this method is briefly presented for the concrete with maximum compressive strength up to 62 MPa. Figure 3 defines the ultimate compressive stress ( $\sigma_{cu}$ ), strain at  $\sigma_{cu}$  ( $\varepsilon_0$ ) and the strain corresponding to the stress at  $0.3\sigma_{cu}$  in the descending portion ( $\varepsilon_d$ )[18, 19]. A linear stress-strain relationship, which obeys Hooke's law, is assumed up to 50% of the ultimate compressive strength ( $\sigma_{cu}$ ) in the ascending portion [20].



**Figure 3.** Model developed by Hsu and Hsu for compressive behavior of concrete[17]

The numerical model by Hsu and Hsu (1994) is merely utilized to compute the compressive stress values ( $\sigma_c$ ) at  $0.5\sigma_{cu}$  (yield point) and  $0.3\sigma_{cu}$  in the descending portion. Its formula is described as follow (1):

$$\sigma_c = \left( \frac{\beta \left( \frac{\varepsilon_c}{\varepsilon_0} \right)}{\beta - 1 + \left( \frac{\varepsilon_c}{\varepsilon_0} \right)^\beta} \right) \quad (1)$$

Where, the parameter  $\beta$ , which depends on the form of the stress-strain diagram, is derived from (2) and the strain at the  $\sigma_{cu}$  (peak stress)  $\varepsilon_0$  is given by (3):

$$\beta = \frac{1}{1 - \left( \frac{\sigma_{cu}}{\varepsilon_0 \times E_0} \right)} \quad (2)$$

$$\varepsilon_0 = (8.9 \times 10^{-5} \sigma_{cu}) + (2.114 \times 10^{-3}) \quad (3)$$

The elasticity modulus,  $E_0$  is given by (4):

$$E_0 = (1.2431 \times 10^2 \sigma_{cu}) + (3.28312 \times 10^3) \quad (4)$$

It should be noted that  $\sigma_c$ ,  $\sigma_{cu}$  and  $E_0$  are in kip/in<sup>2</sup> in the above equations.

The  $\varepsilon_d$  is iteratively calculated using (5) when  $\sigma_c=0.8\sigma_{cu}$ .

The model developed by Nayal and Rashid (2006) [21] is adopted to demonstrate the tensile behaviour of concrete (Figure 4).

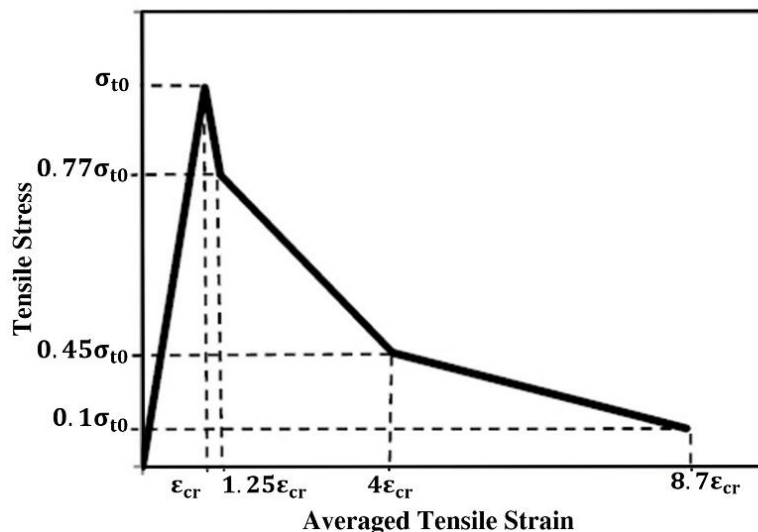


**Figure 4.** Model developed by Nayal and Rashid for tensile behavior of concrete[21]

The main parameters of concrete for elastic and inelastic behavior are illustrated in Table 1.

#### 4.2. Material Characteristics of Masonry Wall

Linear at elastic as well as nonlinear damaged plasticity model for inelastic moods of the masonry wall is considered. Hemant et al.(2007) [22] and Nayal and Rasheed (2006) [21] models are adopted to model the material behavior of masonry wall under compression and tensile. The formula of the stress-strain relations of masonry wall in Hemant et al. (Figure 5) model is expressed as follow:

$$\frac{f_m}{f'_m} = \left( 2 \times \frac{\varepsilon_m}{\varepsilon'_m} \right) - \left( \frac{\varepsilon_m}{\varepsilon'_m} \right)^2 \quad (5)$$

Where,  $f_m$  is the indicator of compressive stress and  $\varepsilon_m$  is the strain in masonry.  $\varepsilon'_m$  is the peak strain corresponding to  $f'_m$ . The nonlinear diagram is more extended in the descending section than  $f'_m$  falls to 90%, after which the curve is simplified as a direct line up to the remaining stress in the masonry wall is attained ( $0.2f'_m$ ), as shown in Figure 5. The following equation is proposed for the assessment of  $\varepsilon'_m$  and  $f'_m$ :

Table 1: Material properties for concrete

Parameter	Value
<b>Elastic properties:</b>	
- Modulus of Elasticity (Mpa)	28284.27
- Density (kgr/m <sup>3</sup> )	2400
- Poisson ratio	0.2
<b>Inelastic properties:</b>	
- Dilation Angle (Degree)	35
- Fbo/Fco	1.16
- flow stress ratio (k)	0.67
- viscosity parameter	0.001

$$\varepsilon'_m = \frac{0.27 \times f'_m}{f_j^{0.25} \times E_m^{0.7}} \quad (6)$$

$$f'_m = 0.63 \times f_b^{0.49} \times f_j^{0.39} \quad (7)$$

It should be noted that the  $E_m$  values assessment using the following equation:

$$E_m = 550 \times f'_m \quad (8)$$

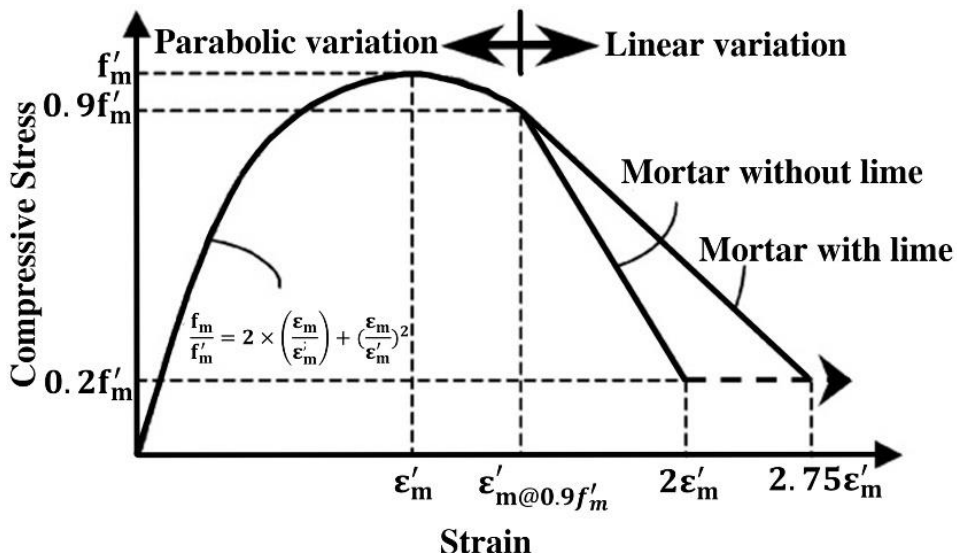


Figure 5. Analytical model for stress-strain curves for compressive behavior of masonry[22]

The model developed by Nayal and Rashid (2006) [21] is chosen and adopted to represent the behaviour of masonry wall under tension.

#### 4.3. Material Characteristics of Steel

For reinforced steel elastic-perfectly plastic behavior in both tension and compression defined. To define the interaction between concrete and reinforcing bar constrain called “embedded region” is used. This constrains prevents any movement of the reinforcing bar inside the concrete. In fact, non-slip reinforcement in concrete to be embedded. The mechanical properties of reinforcing bar adopted in this paper has been shown in Table 2.

**Table 2. Material Properties of Steel**

Parameter	value
<b>Elastic properties:</b>	
-Modulus of Elasticity (Mpa)	210000
-Density (kg/m <sup>3</sup> )	7800
-Poisson ratio	0.3
<b>Plastic properties:</b>	
-Yield stress (Mpa)	300
-plastic strain	0

#### 4.4. Element Section and Mesh Generation

ABAQUS software supplies an extensive range of elements enabling the user to model different geometries and analysis types. The concrete frame and masonry wall were modelled by the use of linear 8-node, reduced integration, hourglass control (C3D8R), and 3D solid elements. The reason for choosing C3D8R elements is that they are considerably appropriate for examining finite strain and rotation in the large-displacement analysis. These elements are also useful for nonlinear static and dynamic analyses[23]. The embedded steel bar is modelled by a 2-node linear beam in space. Mesh size is approximately 200mm for the RC frame and infills. It is approximately 100mm for steel bar.

#### 5. Verification of In-filled RC Frame

Lila Abdolhafez et al. [13] performed a series of experimental tests on the RC frame with different types of infilled wall under monotonic load. The testing program was conducted in three phases. The first phase was conducted on individual reinforced concrete bare frame as a control frame [13]. In the second phase, tests were performed on two types of infilled RC frames. In the first type, the wall was constructed before casting the two columns and the upper beam, and in the second, the columns and beam were constructed and then infilled with masonry [13]. In the third phase, several techniques were used retrofit infilled RC frame in order to improve its seismic performance [13]. More in details, the static tests, which were characterized with monotonic increasing load at the top beam of the frame, were performed to investigate the ductility, toughness, ultimate failure load and pattern of cracks, as well as failure mode [13].

Figure 6 (a) indicates dimensions of the RC frame and Figure 6 (c) shows the Reinforcement detailing of RC frame For masonry unites, the uniaxial strength of the concrete is 350 kg/cm<sup>2</sup>, and the compressive strength is and 75 kg/cm<sup>2</sup>[13]. Table 3 illustrates the mechanical properties of the applied steel bars [13].

**Table 3. Mechanical Properties of Steel Bars [16]**

Bar diameter (mm)	8 mm	12 mm
Yield strength (kg/cm <sup>2</sup> )	2720	5150
Ultimate strength (kg/cm <sup>2</sup> )	4500	7475
% Elongation at failure	26%	23%
Modulus of elasticity (kg/cm <sup>2</sup> )	$2.06 \times 10^6$	$2.06 \times 10^6$

The experimental results have been used as a base for comparison in the following numerical analysis. The results of finite element model analysis (FEA) and the results of the experimental test are compared (Fig. 6(b) and Fig. 6(d)., Load-displacement behavior and ultimate tensile damage, which were constructed from the FEM, were compared with the corresponding ones from experimental testing in order to assess the adequacy of the FEA in estimating the response of masonry infilled frames. As shown in Fig. 6(b) and Fig. 6(d), there is an acceptable agreement between the

experimental and numerical results. Therefore, finite element model was able to adequately predict the behavior of masonry infilled RC frame.

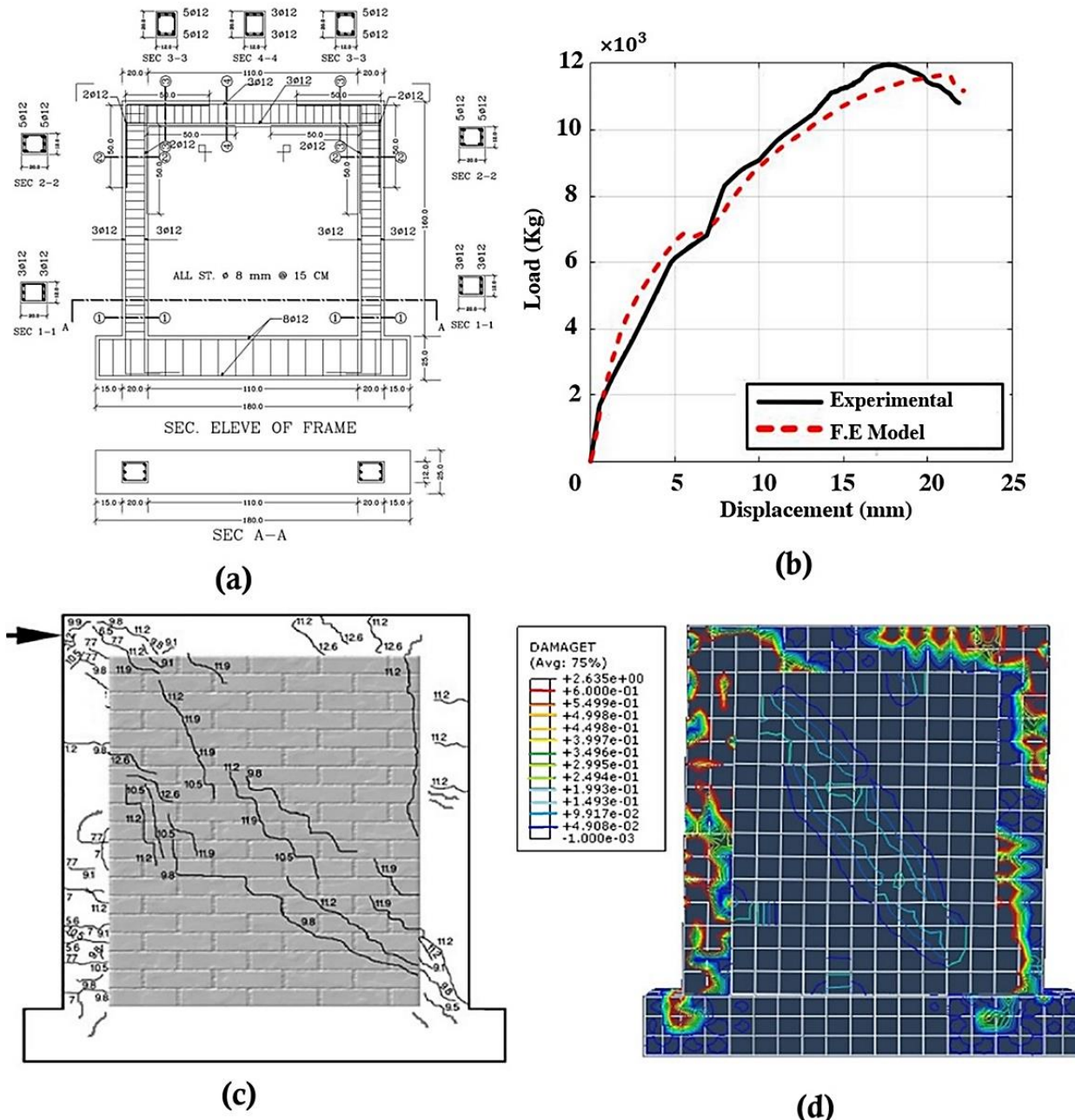


**Figure 6.** (a) Frame Reinforcement Detailing and Dimensions [13]. (b) Load-displacement Comparison between FE Model and Experimental Result. Ultimate tensile Damage between (c) Experimental and (d) FE Model

## 6. Analysis Result and Discussion

Finite element analysis can create very large amounts of output. In order to show the results, this study used two different methods, namely, load-displacement curve and the contour plot. A colorful contour plot products color roll bandages on the numerical model, according to the amounts found in the outcomes file. In order to have a better understanding of the performance of the masonry wall in RC frames, the numerical results of contour plot and load-displacement curve methods are compared in terms of general behavior, pattern of cracks, force transfer mechanisms, lateral load-displacement relationship and resistance, ductility, initial stiffness, and toughness.

### 6.1. Pattern of Cracks

The infilled walls change the behavior of the frames, particularly the way and the process of cracking in RC frames. The cracking is created due to the excessive tensile strength of ultimate tensile strength. Figure 7b shows the tensile cracks in numerical samples under the lateral loading in the Abaqus software. In these figures, the amount of cracking under the tensile force is described by an option located in the left part of the viewport toolbar.

In the first stages of loading, border cracks were created in the line of connection between the frame and infill wall of the infilled frame without opening. Then, hairline cracks were formed in the column and extended along it. In the mid-height of masonry infill wall, the horizontal cracks were formed under the increase of lateral load and continued to compressive corners. As the loading continues, the columns suffer from shear failure along diagonal cracks. As a matter of course, these cracks were located exactly at the distance between the stirrups. As the loading started on infill walls with opening, the border cracks were first formed, and then hairline cracks extended in the column. With the increment of lateral loading, some cracks were observed in the opening corner and directed to compressive corners. Similar to infilled RC frame without opening, in models with windows of high tensile cracks were observed in the column. Formation of shear cracks in columns was a significant point in infilled RC frame. Unlike bar frames, in infilled RC frames, these sorts of cracks (i.e., shear cracks) were created parallel and near to the infill walls and in one direction. Hence, it could be concluded that the interaction among masonry infilled wall and RC frame created such a pattern. In other words, shear stress has been increased by separating masonry infilled wall from the RC frame in the stressed diagonal.

## 6.2. Force Transfer Mechanisms

When a frame with infilled wall is impacted by a lateral force in its panel, the infill wall prevents flexural action in the frame making an interaction among the RC frame and masonry infilled wall. Due to the interaction among masonry infilled wall and RC frame, infilled wall transfers some of the load exerted by the building. Therefore, this infilled wall is considered as a part of building's force resisting system. The significant question would be arisen is that "what would be the transfer direction of the load if there was a masonry infilled wall in the RC frame?" In order to answer this question, we used the counters of principal stress ( $S_{\text{min}}$ ,  $S_{\text{min}}$ , Principal). Figure 7(a) indicates force transfer mechanism under one direction load in Abaqus software.

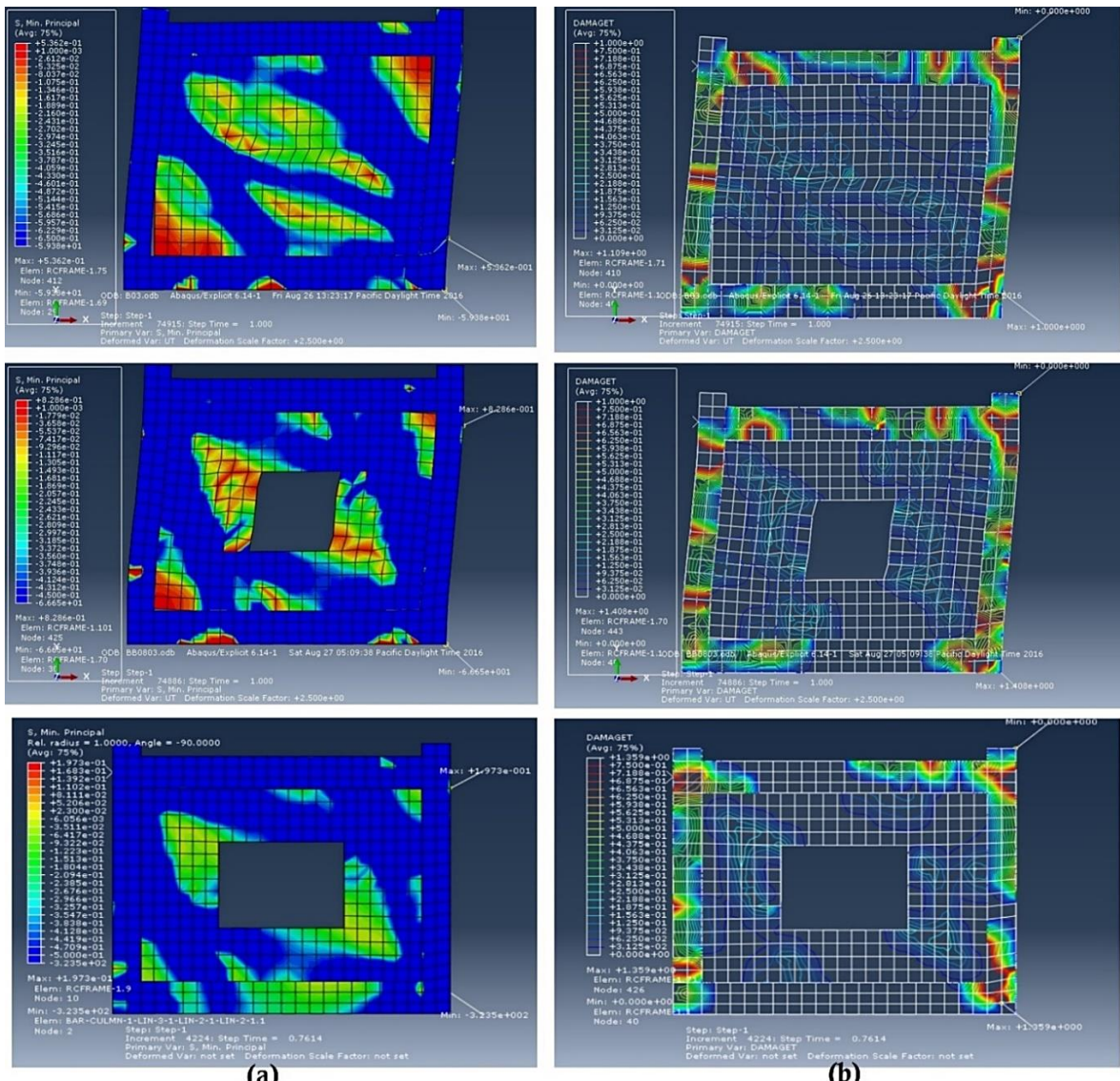


**Figure 7. Force transfer mechanism and tensile damage patterns of infilled frames: (a) plots of the principal compressive stress distributions of infilled frames (b) ultimate tensile damage in infilled frames**

As shown in Figure 7(a), in the frames with infilled wall without opening, compressive stresses are in maximum levels on diagonal tensile, corner, and along the four sides of the infill-to-frame connection. Tensile stresses are maximum in both ends but minimum in the middle (center). Figure 7(a) also shows that opening increases tensile stresses on compressive diagonal in opening corners and extends them toward loaded corners. It should be mentioned that, in all numerical models, the average of tensile stress is much less than compressive stress in the infilled wall. Comparing the stress distributed in bar frame and infilled frames, it could be concluded that a large compressive force has been transferred from infilled walls to columns. The exerted force on columns, which is due to the interaction between frame and infilled wall, could develop plastic regions in the columns. In other words, the presence of infilled wall could jeopardize the mechanism of Strong Column - Weak Beam. Therefore, it is essential to control beam and surrounding columns against forces caused by infilled wall and frame interaction.

## 6.2. Lateral Load-displacement Relationship and Ultimate Load

Figure 8 illustrates the lateral load-displacement curves of models. Table 4 shows the ultimate load of all models as well as the ratio of ultimate loads to the control frame (bare frame).

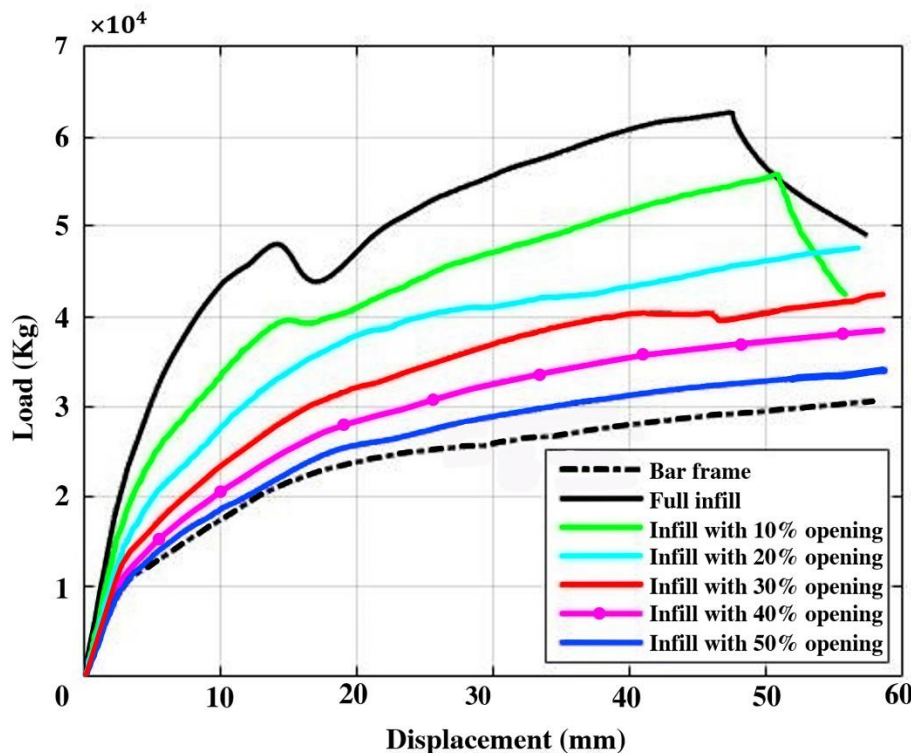


**Figure 8. The Lateral load-displacement Curves**

**Table 4. the Numerical Values of Ultimate Loads**

Models	P <sub>u</sub> (ton)	P <sub>u</sub> / P <sub>u bare</sub>
Bar frame	30.541	1
Full infill	62.755	2.05
Infill with 10% opening	55.636	1.821
Infill with 20% opening	47.760	1.563
Infill with 30% opening	42.313	1.385
Infill with 40% opening	38.430	1.258
Infill with 50% opening	33.943	1.111

-The effect of infilled wall

Because of the inevitable interaction among the RC frame and the masonry infilled wall, ultimate loads for infilled frame are higher than the corresponding bar frame.

-The effect of opening

For windows opening with a surface area of 10% of the infill wall area, the increase in ultimate loads was more than

for the cease of windows opening with a surface area of 20%. Also presence of opening within infilled RC frame led to the decrease of ultimate loads corresponding full infill, as well as increasing of opening size led to increasing the reduction of the ultimate loads.

### 6.3. Ductility

Figure 8 shows the lateral load-displacement Lateral load-displacement provide us with significant data on the ultimate displacement of the masonry infilled RC frames, which are helpful for specifying seismic parameter, such as ductility [24]. The ductility  $\mu$  is defined as the ratio among yield and ultimate displacement[24]. The following equation expresses ductility as:

$$\mu = \frac{\delta_u}{\delta_y} \quad (9)$$

Table 5 shows values of pseudo ductility.

**Table 5. The Ductility and Its Ratio to the Control Frame (Bar Frame)**

Models	D <sub>u</sub>	D <sub>u</sub> /D <sub>u,bare</sub>
Bar frame	8.28	1
Full infill	6.44	0.77
Infill with 10% opening	5.8	0.70
Infill with 20% opening	7.25	0.87
Infill with 30% opening	6.44	0.77
Infill with 40% opening	6.53	0.78
Infill with 50% opening	7.37	0.89

From this table, it can be seen that:

- The effect of infilled wall

Ductility of full infilled frame has the least value in comparison bar frame. This is ascribed to the existence of the masonry infilled wall.

- The effect of opening

The presence of opening within in-filled RC frame led to the decrease of ductility corresponding full infill, as well as increasing of opening size led to increasing the reduction of the ductility. As shown in Table 3, there is no significant difference between the initial ductility of full infill and the windows opening infill.

### 6.4. Initial Stiffness

Overlooking the effect of infill walls does not always increase the confidence in structural design. The distance between center of rigidity and center of mass could be increased due to the increase of stiffness caused by infill walls, and it would contribute into destructive torsions in building for which torsion has been neglected during the symmetric design. Thus, it is required to examine the impacts of infilled walls on stiffness despite the ignorance of their resistance. Stiffness is the rigidity of a structural element the extent to which it resists plastic deformation against applied load [9]. The initial stiffness of every numerical model was calculated by displacement-based design (DBD) method [18] described as follow:

$$K = \frac{F_y}{\delta_y} \quad (10)$$

Where F<sub>y</sub> the yielding is load and δ<sub>y</sub> is yielding drift. Table 6 shows the value of initial stiffness for all numerical models. According to Table 6, it can be seen that:

- The effect of infilled wall

The existence of the masonry infilled wall considerably increases the initial stiffness of the infilled RC frames.

- The effect of opening

Presence of opening within infilled RC frame decreased the stiffness corresponding to full infill frame. This is attributed to the increasing damage in the infill. It should be noted here that the increase of opening size reduced the stiffness.

**Table 6. the initial stiffness and Its Ratio to the Control Frame (Bar Frame)**

Models	$K$ (ton/mm)	$K/K_{bare}$
Bar frame	2.92	1
Full infill	6.44	2.20
Infill with 10% opening	5.186	1.77
Infill with 20% opening	4.152	1.42
Infill with 30% opening	3.425	1.17
Infill with 40% opening	2.96	1.013
Infill with 50% opening	2.95	1.01

### 6.5. Toughness

The toughness is considered as one of the utmost significant aspects in examining the performance of infilled RC frames under various loading conditions [24]. Toughness is the capability of a structural element in absorption of energy and large deformation without failure [24]. The toughness is viewed as the area under the load-displacement diagram for each numerical model [24]. Table 7 shows the results of the values of toughness (ton.mm).

**Table 7. the Toughness and its Ratio to the Control Frame (Bar Frame)**

Models	$Tou$ (ton.mm)	$Tou/Tou_{bare}$
Bar frame	1370.922	1
Full infill	2872.013	2.09
Infill with 10% opening	2453.68	1.78
Infill with 20% opening	2157.842	1.57
Infill with 30% opening	1931.962	1.4
Infill with 40% opening	1735.153	1.26
Infill with 50% opening	1538.73	1.12

The study of table indicates that:

-The effect of infilled wall

It is clear that the existence of infilled wall increases the toughness. This is due to the presence of the masonry wall in RC frames.

-The effect of opening

As shown in table 5, the presence of opening with the infilled wall reduced the toughness of the infilled system in comparison to the full infilled frame. It should be noted here that the increasing of opening size led to increasing the reduction of toughness.

## 7. Conclusions

In this paper, seven full-scale, one-story and one-bay RC frame, namely, a bar frame, a fully in-filled frame, in-filled frame with 10%, 20%, 30%, 40% and 50% window opening respectively under monotonic horizontal load were investigated. According to the analysed results, the following conclusions could be drawn:

- The ultimate loads for full in-filled frame are higher than the corresponding bar frame by about 105%. Furthermore, the ultimate loads for infills with 10%, 20%, 30%, 40%, 50% openings are greater than bar frame about 82%, 56%, 38%, 25% and 11%, respectively. It means that the presence of windows opening within in-filled RC frame raised the ultimate loads, which are corresponded to bar frame. Hence, the increase of opening size increased the reduction of the ultimate loads.
- Ductility of full in-filled frame has the less value than the bar frame, which is about 33%.
- The initial stiffness for full in-filled frame are higher than the corresponding bar frame by about 120%. Furthermore, the initial stiffness for infill with 10%, 20%, 30%, 40%, 50% opening are greater than bar frame

about 77%, 42%, 17%, 1.3% and 1%, respectively. It means that the masonry infilled wall increases the stiffness of the RC frames; however, the existence of windows opening within the infilled wall reduces the stiffness.

- The toughness for full in-filled frame are higher than the corresponding bar frame by about 109%. Furthermore, the lateral stiffness for infill with 10%, 20%, 30%, 40%, 50% opening are greater than bar frame about 78%, 57%, 40%, 26% and 12%, respectively. It means that the toughness for full infilled frame are higher than the corresponding bar frame. In addition, the presence of opening within in-filled RC frame decreased the toughness, which is corresponded to full infill. The increasing of opening size increased the reduction of the toughness.
- The infilled walls in concrete frame exert much compression on the base beam leading to split in the beam-column joint. The more increase in opening dimension size, the less compression on the base beam. Furthermore, additional closed stirrups are also used to prevent splitting column in the location of column – beam connection.

## 8. Conflicts of Interest

The authors declare no conflict of interest.

## 9. References

- [1] S. S. Ravichandran, "Design provisions for autoclaved aerated concrete (AAC) infilled steel moment frames," 2009.
- [2] A. Furtado, H. Rodrigues, and A. Arêde, "Modelling of masonry infill walls participation in the seismic behaviour of RC buildings using OpenSees," International Journal of Advanced Structural Engineering (IJASE), vol. 7, pp. 117-127, 2015. DOI 10.1007/s40091-015-0086-5.
- [3] I. R. Hapsari, S. Sangadji, and S. A. Kristiawan, "Seismic performance of four-storey masonry infilled reinforced concrete frame building," in MATEC Web of Conferences, 2018, p. 02017. doi:10.1051/matecconf/201819502017.
- [4] H. Alwashali, Y. Torihata, K. Jin, and M. Maeda, "Experimental observations on the in-plane behaviour of masonry wall infilled RC frames; focusing on deformation limits and backbone curve," Bulletin of Earthquake Engineering, vol. 16, pp. 1373-1397, 2018. doi:10.1007/s10518-017-0248-x.
- [5] S. H. Basha and H. B. Kaushik, "Behavior and failure mechanisms of masonry-infilled RC frames (in low-rise buildings) subject to lateral loading," Engineering Structures, vol. 111, pp. 233-245, 2016. doi:10.1016/j.engstruct.2015.12.034.
- [6] X. Chen and Y. Liu, "A finite element study of the effect of vertical loading on the in-plane behavior of concrete masonry infills bounded by steel frames," Engineering Structures, vol. 117, pp. 118-129, 2016. doi:10.1016/j.engstruct.2016.03.010.
- [7] A. Kiani, B. Mansouri, and A. S. Moghadam, "Fragility curves for typical steel frames with semi-rigid saddle connections," Journal of Constructional Steel Research, vol. 118, pp. 231-242, 2016. doi:10.1016/j.jcsr.2015.11.001.
- [8] Y. Yuen and J. Kuang, "Nonlinear seismic responses and lateral force transfer mechanisms of RC frames with different infill configurations," Engineering Structures, vol. 91, pp. 125-140, 2015. doi:10.1016/j.engstruct.2015.02.031.
- [9] A. S. A. T. Essa, M. R. K. Badr, and A. H. El-Zanaty, "Effect of infill wall on the ductility and behavior of high strength reinforced concrete frames," HBRC Journal, vol. 10, pp. 258-264, 2014. doi:10.1016/j.hbrcj.2013.12.005.
- [10] D. Okuyucu, "Effects of frame aspect ratio on the seismic performance improvement of panel strengthening technique," Ph. D. thesis, Middle East Technical Univ., Ankara, Turkey, 2011.
- [11] R. S. O. Keskin, "Behavior of Brick Infilled Reinforced Concrete Frames Strengthened by Cfrp Reinforcement: Phase I," 2002.
- [12] M. Baran and T. Sevil, "Analytical and experimental studies on infilled RC frames," International Journal of Physical Sciences, vol. 5, pp. 1981-1998, 2010.
- [13] L. M. Abdel-Hafez, A. Abouelezz, and F. F. Elzefary, "Behavior of masonry strengthened infilled reinforced concrete frames under in-plane load," HBRC Journal, vol. 11, pp. 213-223, 2015. doi:10.1016/j.hbrcj.2014.06.005.
- [14] E. Patelli, M. Beer, S.-K. Siu-Kui Au, and I. A. Kougioumtzoglou, Encyclopedia of earthquake engineering: Springer, 2015.
- [15] W. Van der Mersch, "Modelling the seismic response of an unreinforced masonry structure," 2015.
- [16] P. Grassl and M. Jirásek, "Damage-plastic model for concrete failure," International journal of solids and structures, vol. 43, pp. 7166-7196, 2006. doi:10.1016/j.ijsolstr.2006.06.032.
- [17] L. Hsu and C.-T. Hsu, "Complete stress—strain behaviour of high-strength concrete under compression," Magazine of concrete research, vol. 46, pp. 301-312, 1994. Author Affiliations. doi:10.1680/macr.1994.46.169.301.
- [18] A. M. Morsy, N. H. El-Ashkar, and I. S. Mattar, "Nonlinear finite element modeling of reinforced concrete beams in shear-strengthened with near surface mounted laminates," Concrete Solutions 2014, p. 321, 2014.
- [19] A.-T. Le, T.-Q. Hoang, and T.-T. Nguyen, "Analysis Behavior of Reinforcement in a Reinforced Concrete Beam Using Steel Slag Replacing Crushed-Stone Aggregate," in Congrès International de Géotechnique—Ouvrages—Structures, 2017, pp. 329-337. doi:10.1007/978-981-10-6713-6\_32.
- [20] B. Dastjerdy, R. Hasanpour, and H. Chakeri, "Cracking Problems in the Segments of Tabriz Metro Tunnel: A 3D Computational

- Study," *Geotechnical and Geological Engineering*, vol. 36, pp. 1959-1974, 2018. doi:10.1007/s10706-017-0439-x.
- [21] R. Nayal and H. A. Rasheed, "Tension stiffening model for concrete beams reinforced with steel and FRP bars," *Journal of Materials in Civil Engineering*, vol. 18, pp. 831-841, 2006. doi:10.1061/(ASCE)0899-1561(2006)18:6(831).
- [22] H. B. Kaushik, D. C. Rai, and S. K. Jain, "Uniaxial compressive stress-strain model for clay brick masonry," *Current Science*, pp. 497-501, 2007.
- [23] A. Ahmed, "Modeling of a reinforced concrete beam subjected to impact vibration using ABAQUS," *International journal of civil and structural engineering*, vol. 4, p. 227, 2014. doi: 10.6088/ijcser.201304010023.
- [24] A. Akhaveissy and G. Milani, "Pushover analysis of large scale unreinforced masonry structures by means of a fully 2D non-linear model," *Construction and Building Materials*, vol. 41, pp. 276-295, 2013. doi:10.1016/j.conbuildmat.2012.12.006.